

## ARTICLE

# Multigenic lentiviral vectors for combined and tissue-specific expression of miRNA- and protein-based antiangiogenic factors

Anne Louise Askou<sup>1</sup>, Lars Aagaard<sup>1</sup>, Corinne Kostic<sup>2</sup>, Yvan Arsenijevic<sup>2</sup>, Anne Kruse Hollensen<sup>1</sup>, Toke Bek<sup>3</sup>, Thomas Gryesten Jensen<sup>1</sup>, Jacob Giehm Mikkelsen<sup>1</sup> and Thomas Juhl Corydon<sup>1</sup>

Lentivirus-based gene delivery vectors carrying multiple gene cassettes are powerful tools in gene transfer studies and gene therapy, allowing coexpression of multiple therapeutic factors and, if desired, fluorescent reporters. Current strategies to express transgenes and microRNA (miRNA) clusters from a single vector have certain limitations that affect transgene expression levels and/or vector titers. In this study, we describe a novel vector design that facilitates combined expression of therapeutic RNA- and protein-based antiangiogenic factors as well as a fluorescent reporter from back-to-back RNApolIII-driven expression cassettes. This configuration allows effective production of intron-embedded miRNAs that are released upon transduction of target cells. Exploiting such multigenic lentiviral vectors, we demonstrate robust miRNA-directed downregulation of vascular endothelial growth factor (VEGF) expression, leading to reduced angiogenesis, and parallel impairment of angiogenic pathways by codelivering the gene encoding pigment epithelium-derived factor (PEDF). Notably, subretinal injections of lentiviral vectors reveal efficient retinal pigment epithelium-specific gene expression driven by the VMD2 promoter, verifying that multigenic lentiviral vectors can be produced with high titers sufficient for *in vivo* applications. Altogether, our results suggest the potential applicability of combined miRNA- and protein-encoding lentiviral vectors in antiangiogenic gene therapy, including new combination therapies for amelioration of age-related macular degeneration.

*Molecular Therapy — Methods & Clinical Development* (2015) **2**, 14064; doi:10.1038/mtm.2014.64; published online 28 January 2015

## INTRODUCTION

Intraocular neovascular diseases are the leading cause of blindness in the Western world in individuals over the age of 50. Exudative age-related macular degeneration (AMD) is one of these diseases and is characterized by aberrant neovessel development, sprouting from the choroidal vessels into the subretinal space through a fragmented Bruch's membrane. Without treatment such new vessel formation, called choroidal neovascularization (CNV), can cause irreversible damage to the vulnerable photoreceptor cells essential for high-resolution, central vision. The advent of anti-vascular endothelial growth factor (VEGF) therapy has markedly changed the outcome of treatment, and the success has positioned VEGF at the epicenter of research for new treatment modalities for retinal vascular diseases.

Despite the high success rate, clinicians still examine eyes that are only partially responsive or even nonresponsive to antibody-based anti-VEGF therapy, underscoring the need for a new and refined treatment. Recently, several studies have been published, examining the outcome of combined or triple therapy for the treatment of exudative AMD.<sup>1–3</sup> The rationale behind utilization of combination therapies relates to the different mechanism of action of the combined therapies. The complexity of pathogenic neovascularization, including the numerous complex pathways mediating the effect of

VEGF, indicates that simultaneous targeting of different pathways of this process may have synergistic effects and thus improve visual outcome and/or reduce treatment frequency.

The potential of RNA interference (RNAi) therapy for a broad range of diseases has led to clinical trials evaluating the safety and efficacy of three short interfering RNAs (siRNA) for treatment of exudative AMD.<sup>4–6</sup> The safety data have been encouraging, but phase II and III clinical trials testing AGN211745 and bevasiranib, respectively, were terminated due insufficient efficacy of the siRNA monotherapy. However, combined therapy of ranibizumab and siRNA was found to be superior to ranibizumab monotherapy, which is currently the standard treatment.<sup>7,8</sup> In these trials, naked siRNA was delivered by intravitreal injections with the drawback of multiple injections just as conventional treatments. Another concern regarding siRNA-based therapy was raised when it was discovered that suppression of CNV does not occur through the specific action of the siRNA targeting VEGF, but rather as a generic, sequence-independent property of the noninternalized siRNAs.<sup>9</sup>

We and others have previously shown, that anti-VEGF short hairpin RNAs (shRNAs) encoded by viral vectors can reduce CNV in mice following a single injection.<sup>4,10,11</sup> Additionally, we have shown that adenoassociated viral (AAV)-mediated delivery of an anti-VEGF microRNA (miRNA) cluster can knockdown endogenous VEGF

<sup>1</sup>Department of Biomedicine, Aarhus University, Aarhus, Denmark; <sup>2</sup>Department of Ophthalmology, Unit of Gene Therapy and Stem Cell Biology, University of Lausanne, Jules-Gonin Eye Hospital, Lausanne, Switzerland; <sup>3</sup>Department of Ophthalmology, Aarhus University Hospital, Aarhus, Denmark. Correspondence: TJ Corydon (corydon@biomed.au.dk)  
Received 20 August 2014; accepted 10 December 2014

in a mouse model.<sup>12</sup> To achieve synergy in a genetic intervention approach, we explore in this study means of combining RNAi-based silencing of VEGF, which is upregulated during pathological conditions, with delivery of therapeutic proteins. Such proteins could be antiangiogenic, antiinflammatory, or for instance neurotrophic such as the protein pigment epithelium-derived factor. We engineer multigenic LV vectors and demonstrate the potential of combining multiple miRNAs with protein expression for combined antiangiogenic activity. We show efficient knockdown of VEGF *in vitro* and provide *in vivo* evidence for localized transgene expression following incorporation of the retinal pigment epithelium-specific vitelliform macular dystrophy 2 (VMD2) promoter into the vector. These results have potential implications for the future development of gene delivery vehicles for combination therapy of neovascular diseases, including exudative AMD.

## RESULTS

Multigenic LV vectors are functional and versatile gene delivery vehicles

We generated multigenic LV constructs by inserting an additional AsRed-encoding expression cassette in reverse orientation in a pCCL-based LV transfer plasmid, here designated pLV/PE (Figure 1a). Between the promoter and the AsRed coding sequence, we inserted a modified  $\beta$ -globin intron containing a linker sequence for insertion of intronic miRNA clusters. Effective and precise splicing of the pre-mRNA was confirmed by PCR. Primers were designed to bind in the 5' exon region of the  $\beta$ -globin exon-intron-exon sequence and in the region of a red fluorescent protein, AsRED (Figure 1a), amplifying a short fragment of 791 bp indicative of splicing, as opposed to a longer fragment of 1,270 bp in the absence of splicing (Figure 1b). Only the short PCR product was observed when cDNA was used as a template, whereas a longer PCR product was generated in the control using plasmid DNA as template. This indicates correct splicing of the expressing cassette, allowing for processing of the miRNA cluster (see below).

Titer assessment of different LV preparations was performed by flow cytometry analysis of cells transduced with serially diluted viral preparations (Figure 1c) and p24 ELISA (see Materials and Methods). The amount of p24 determined by ELISA for each LV preparation was found to range from  $1.6 \times 10^5$  to  $1.1 \times 10^6$  pg p24/ml, and the effective titer ranged from  $6.2 \times 10^5$  to  $1.6 \times 10^7$  TU/ml. The highest effective titers were obtained for LV/PE, but vectors carrying the CMV-intron cassette were effectively transferred with titers that were reduced up to 12-fold relative to LV/PE. Notably, neither insertion of the triple miRNA encoding sequences in the intron nor the actual sequence of the miRNA insert did not adversely affect the effective titer (Figure 1c).

For RPE-specific expression *in vivo*, the CMV promoter was replaced with the VMD2 promoter. AsRED was inserted to assess cell-specific expression from the VMD2 promoter. Immunofluorescence analysis of eGFP and AsRED expression in three different human cell lines, HEK-293, ARPE-19, and melanoma<sup>13</sup> cells, was investigated 4 days after transduction with LV/VMD2-intron-AsRED-PE (Figure 1d). Robust eGFP expression indicated sufficient transduction of all cell lines, but high levels of AsRED expression were found only in melanoma cells, and not in ARPE-19 cells, indicating profound cell-specific expression from the VMD2 promoter. This finding was not unexpected, since expression levels of transcription factors and the VMD2 gene itself differ significantly in the ARPE-19 cell line compared to primary RPE cells.<sup>14</sup>

These results demonstrated that after transcription the intron was spliced out and a functional protein, in this case AsRED, was produced. Hence, the vector system is highly versatile, and replacement of either transgene or miRNA cluster does not profoundly affect the titer. This allows for easy manipulation of vector elements and tailoring of the vector for a broad range of specific applications.

Multigenic LV vectors efficiently transduce cells in the outer retina following subretinal delivery in mice

Based on the development of a highly versatile LV vector, we wanted to investigate whether the titer obtained for such complex LV vectors was sufficient for *in vivo* transgene expression. To assess transgene expression in the mouse retina, four eyes of mice were injected with 30 ng p24 LV/VMD2-miR(5,8,7)-AsRED-PE (Figure 2). To determine which cells of the retina the LV vectors transduced, frozen sagittal sections of injected retinas were analyzed 21 days after injection by fluorescence microscopy. Robust expression of eGFP and AsRED was evident in the retina but, as expected, limited to the area in vicinity of the injection site (Figure 2a–c). Additionally, a magnified image of the retina depicting eGFP and AsRED signals revealed eGFP expression in transduced cells in the inner and outer nuclear layers including the RPE cells, whereas the AsRED signal was found exclusively in RPE cells in the investigated eyes (compare Figure 2d and 2e). These results demonstrated that the achieved titers of multigenic LV vectors were sufficient for *in vivo* applications and that efficient transgene expression was limited to RPE cells when the expression was driven by the VMD2 promoter following subretinal vector delivery.

miRNAs from the anti-VEGF miR-(5,8,7) cluster are efficiently processed from the LV vectors and can knockdown VEGF

Coexpression of multiple miRNAs from an RNA polymerase II promoter is possible when utilizing a polycistronic miRNA cluster. In a previous study, we have tested the efficacy of shRNA-mediated VEGF knockdown of ten different shRNAs using the dual-luciferase assay, and subsequently generated anti-VEGF miRNA clusters by combining the three most potent target sites in the human VEGF (hVEGF) in an optimized, tricistronic MCM7-based miRNA cluster.<sup>12</sup> In this study, we modified this tricistronic miR-5,10,7 targeting hVEGF<sub>165</sub> to generate the miR(5,8,7) expressing vector targeting murine VEGF<sub>164</sub> (mVEGF) by replacing each of the anti-hVEGF miRNAs with murine targeting anti-mVEGF miRNAs. miR-10 was replaced by miR-B, a miR-93-mimic designed to release a miRNA targeting the same position in mVEGF as bevasiranib<sup>4</sup> (formerly Cand5, OPKO Health), a novel siRNA used for treatment of wet AMD. The HIV-targeting MCM7-based miRNA cluster, miR(S1,S2,S3), was used as an irrelevant, nontargeting negative control (referred to as miR-Irr in this study).<sup>15</sup>

Functional expression of miRNAs from the cluster was tested by cotransfecting HEK-293 cells with pcDNA3.1-based plasmids expressing the different miRNA clusters and the dual luciferase psiCHECK reporter construct, psiCHECK-mVEGF (see Materials and Methods). As shown in Figure 3a, an improved gene silencing effect was observed by combining two or three miRNAs in the cluster. We achieved a significant mVEGF knockdown by all seven miRNA clusters generated in this study compared to miR(Irr) (\**P* < 0.001 for all). Notably, the miR(5,8,7) cluster comprising all three VEGF-targeting miRNAs was able to downregulate the mVEGF reporter by  $78 \pm 2\%$  (\**P* < 0.0001).

Subsequently, the miR(5,8,7) and the miR(Irr) clusters were inserted in the intron of pLV/CMV-intron-AsRED and pLV/

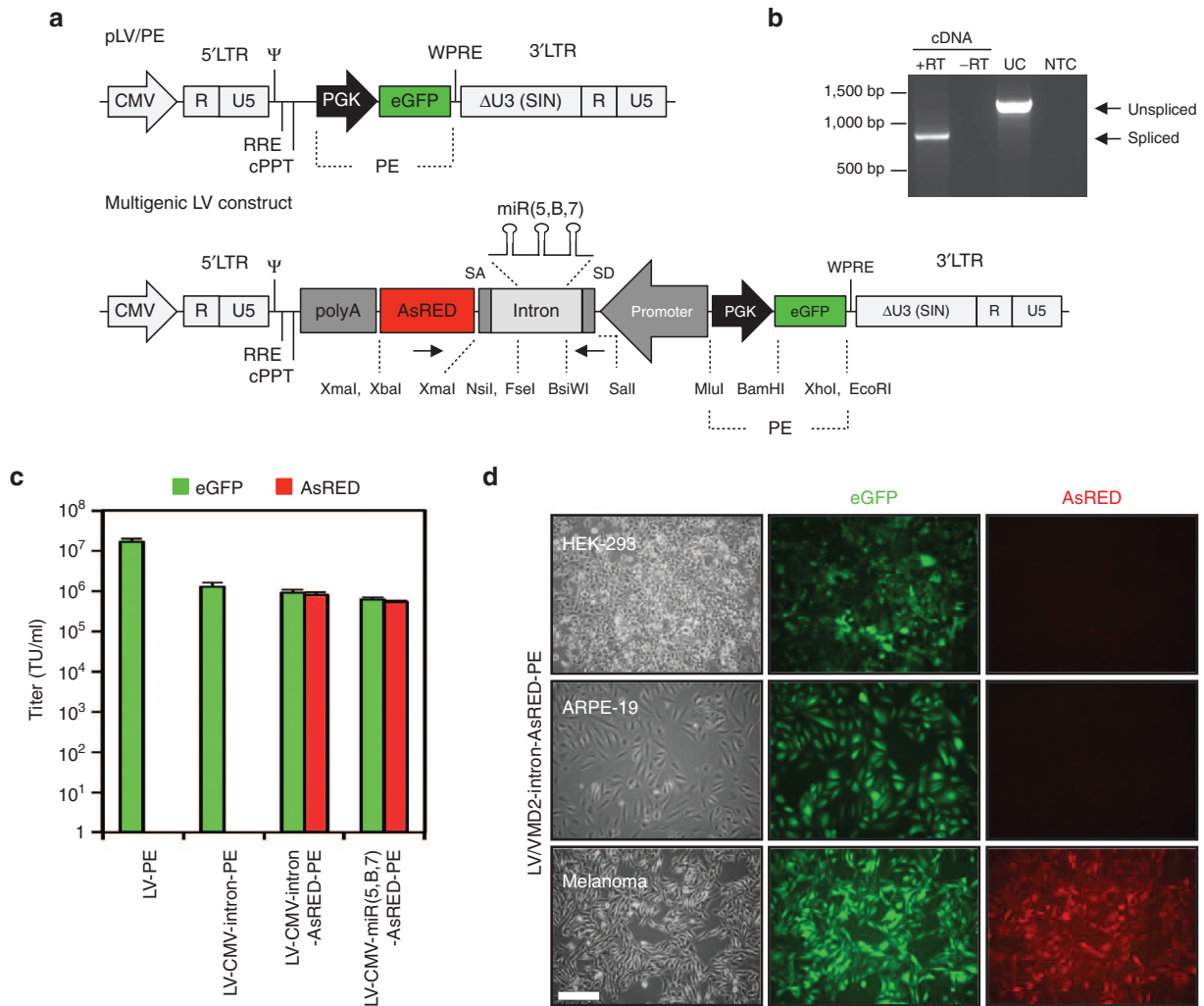


**Figure 1** Design and functionality of the multigenic LV vectors. **(a)** Schematics of the pLV/PE and multigenic LV expression cassettes. The LV transfer vector incorporates a promoter (CMV or the RPE-specific VMD2) that drives the expression of a single mRNA encoding both anti-mVEGF miRNAs (miR(5,B,7)) and a transgene (AsRED or PEDF). If indicated, the LV vectors also encode eGFP driven by the PGK promoter as a reporter gene (PE). Restriction sites used for cloning are shown. Arrows in **a** indicate PCR primer binding sites. **(b)** Assessment of splicing of pre-mRNA by PCR analysis. RNA was purified from HEK-293 cells transduced with LV-CMV-intron-AsRED-PE 48 hours after transduction. Products from cDNA synthesis with (+RT) and without (-RT) reverse transcriptase were used as template in a PCR. If the mRNA is spliced, the expected size of the PCR product is 791 bp. pLV-CMV-intron-AsRED-PE plasmid DNA was used as unspliced control (UC) with a product size expected to be 1,270 bp and H<sub>2</sub>O as nontemplate control (NTC). **(c)** Functional titer determined by flow cytometry analysis of HEK-293 cells (mean ± SD). **(d)** Immunofluorescence analysis of eGFP and AsRED expression in three different cell lines (HEK-293, ARPE-19, and melanoma cells) 4 days after transduction with 100 ng p24 LV-VMD2-intron-AsRED-PE. Scale bar = 100 μm. ARPE-19, human retinal pigment epithelium cells; CMV, cytomegalovirus; cPPT, central polyurine tract; eGFP, enhanced green fluorescent protein; HEK-293, human embryonic kidney cells; LTR, long terminal repeat; LV, lentiviral; -PE, PGK-eGFP; PGK, phosphoglycerate kinase 1 promoter; polyA, bovine growth hormone polyadenylation signal; ψ, packaging signal; RRE, Rev-responsive element; RT, reverse transcriptase; SA, splice acceptor; SD, splice donor; TU, transduction unit; U3 (SIN), Self-inactivating deletion in the U3 region; VMD2, vitelliform macular dystrophy 2 promoter; WPRE, woodchuck hepatitis virus posttranscriptional regulatory element.

VMD2-intron-AsRED constructs, generating the pLV/CMV-miR(5,B,7)-AsRED, pLV/CMV-miR(Irr)-AsRED, pLV/VMD2-miR(5,B,7)-AsRED, and pLV/VMD2-miR(Irr)-AsRED LV transfer plasmids. To test the efficacy of LV-delivered miRNAs, HEK-293 cells were transduced with LV/CMV-miR(5,B,7)-AsRED or LV/CMV-miR(Irr)-AsRED, and melanoma cells were transduced with LV/VMD2-miR(5,B,7)-AsRED or LV/VMD2-miR(Irr)-AsRED. Transduction efficiency was inspected by fluorescence microscopy and revealed strong AsRED expression in the vast majority of the cells as exemplified in Figure 1d. Four days after transduction, cells were transfected with the psiCHECK-mVEGF reporter, and VEGF silencing was assessed by measuring RLuc/PLuc activity in cell extracts. Both promoters,

CMV and VMD2, were able to significantly downregulate VEGF (38 ± 2% and 49 ± 5%, respectively) (Figure 3b).

Correct processing of all three miRNAs from the intron region was verified by northern blotting (Figure 3c). Total RNA was extracted from HEK-293 cells transfected with pcDNA3.1-based plasmids encoding the tricistronic miR(5,B,7), the irrelevant control miR(Irr), or clusters harboring only one of the anti-mVEGF miRNAs and two anti-HIV miRNAs (miR(5,S2,S3), miR(S1,B,S3), or miR(S1,S2,7)). Following polyacrylamide gel electrophoresis, mature miRNAs ~21–23 nt long were visualized using miRNA-specific probes, designated probe 5, B and 7, respectively. Probe B gave rise to a much stronger signal compared to probe 5 and 7. The same hybridization

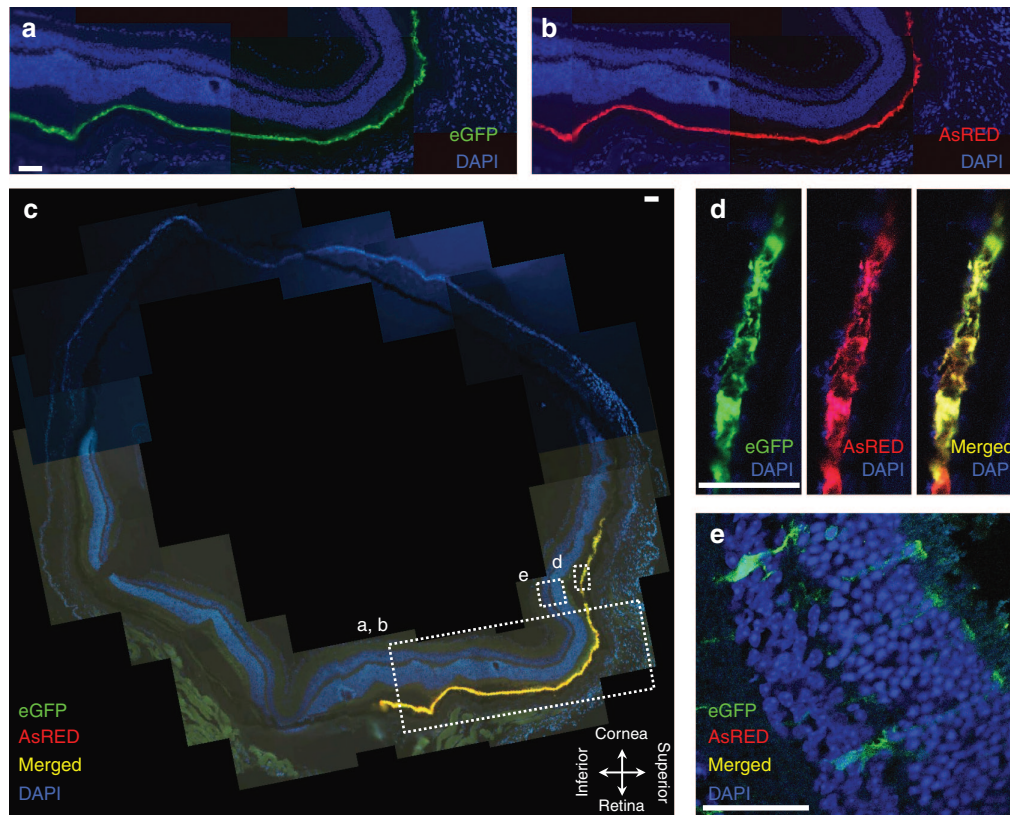


**Figure 2** Histological analysis of LV transduction in the mouse retina 21 days after subretinal injection of 30 ng p24 LV/VMD2-miR(5,B,7)-AsRED-PE. (a) eGFP (green) and (b) AsRED (red) expression in the superior half of the retina, delineated by the large dotted square in c. (c) The sagittal section through the retina is assembled from several individual merged (eGFP and AsRED) illustrations of retinal transduction. The retina is stained with DAPI to show cell nuclei (blue). Expression of eGFP and AsRED reveal localization of LV/VMD2-miR(5,B,7)-AsRED-PE to the RPE cell layer primarily in close vicinity to the injection site located in the superior half of the retina. The areas delineated by the dotted squares are magnified in image a, b, d, and e. Section orientation is shown in the lower right corner. (d) Individual (eGFP and AsRED) and merged images revealing simultaneous expressing of eGFP and AsRED localized to the RPE cell layer, and (e) the inner and outer nuclear layers. The eGFP and AsRED signals are enhanced in e compared to d. Scale bars = 50  $\mu$ m.

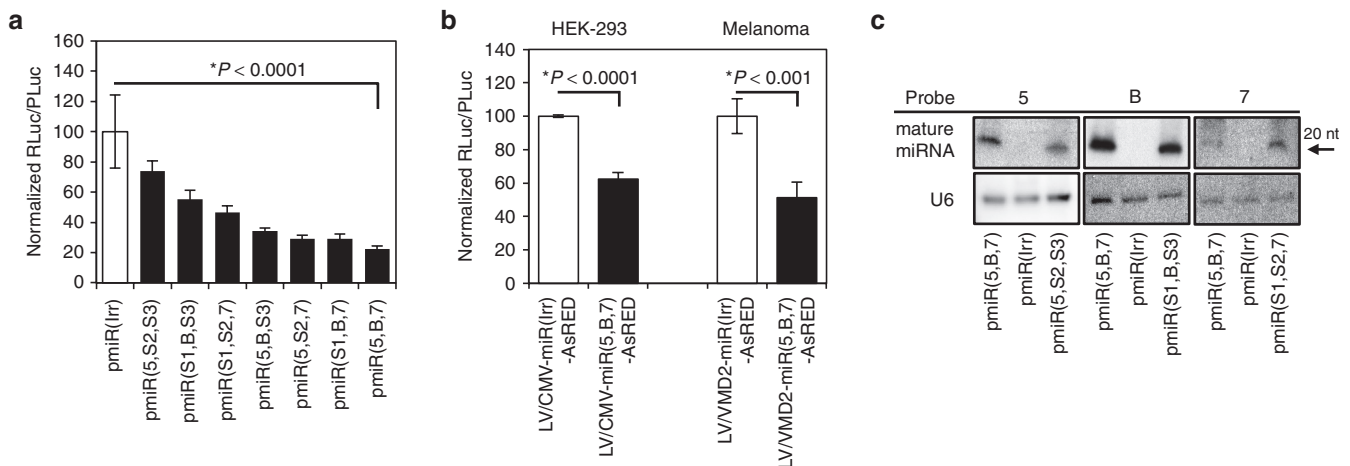


**Figure 3** Expression of miRNAs in HEK-293 and melanoma cells transfected or transduced with miRNA encoding constructs. miRNA-mediated RLuc-VEGF knockdown 48 hours after transfection (a) in cotransfected HEK-293 cells and (b) in LV/CMV-miR(Irr)-AsRED or LV/CMV-miR(5,B,7)-AsRED transduced HEK-293 and LV/VMD2-miR(Irr)-AsRED or LV/VMD2-miR(5,B,7)-AsRED transduced melanoma cells using the dual luciferase assay.  $2 \times 10^5$  HEK-293 cells were transfected with 100 ng p24 LVs corresponding to a MOI of 1.5. Expression of *Renilla* luciferase activity (RLuc) was normalized to the expression of the internal *P. photinus* luciferase (PLuc) as a transfection control and values are presented relative to levels in cells transfected/transduced with miR(Irr) (mean  $\pm$  SD). The decrease in RLuc/PLuc is significant for all miRNA clusters generated compared to miR(Irr). \*Statistically significant. (c) northern blot analysis of 20  $\mu$ g total RNA extract from transfected HEK-293 cells. Mature miRNAs processed from miR(5,B,7) or miR(5,S2,S3), miR(S1,B,S3), and miR(S1,S2,7) were visualized by probe 5, B and 7, respectively. A U6 snRNA-specific probe (U6) was used as a loading control. PLuc, Firefly luciferase; RLuc, *Renilla* luciferase; U6, U6 small nuclear RNA.

conditions were applied for all three probes, and the obvious difference in processed miRNAs detected on the blot possibly reflected suboptimal hybridization conditions for probe 5 and 7, although ineffective processing of the miRNAs by the core machinery of the RNAi pathway could not be ruled out. Similar amounts of miRNA were processed from miR(5,S2,S3), miR(S1,B,S3), or miR(S1,S2,7) compared to miR(5,B,7) (Figure 3c), indicating that miRNA processing was not affected by the sequence of adjacent miRNAs in the cluster.

Our studies of miRNA expression and processing indicate that miRNAs are processed correctly from the intron-based miRNA cluster and are capable of downregulating VEGF expression, when expressed from the versatile LV vector.

#### Inhibition of *in vitro* tube formation by anti-VEGF miRNAs

Following the demonstration of significant VEGF knockdown by miR(5,B,7) in HEK-293 cells, we next wanted to investigate the angiogenic potential of LV-transduced human umbilical vein endothelial cells (HUVECs). The angiogenic potential of LV/CMV-miR(5,B,7)-AsRED-transduced HUVECs was assessed by quantifying the sprouting activity and capillary network complexity in the *in vitro* tube forming assay (Figure 4a). VEGF knockdown by the miR(5,B,7) cluster resulted in significantly smaller cell covered areas, shorter tube length, and fewer branching points and loops after 4 hours than in untransduced and LV/CMV-miR(Irr)-AsRED-transduced HUVECs (Figure 4b). This indicates an overall reduced angiogenic potential due to overexpression of the anti-VEGF miRNAs in HUVECs transduced with LV/CMV-miR(5,B,7)-AsRED. Furthermore, the data suggest that miRNA expression easily can be indirectly assessed by the concomitant AsRED expression from our LV constructs, since significant inhibition of VEGF-mediated tube formation and red

fluorescence was found in cells simultaneously (Figure 4a, lower panel).

#### Pigment epithelium-derived factor expression from the versatile LV vectors

The AsRED gene was replaced with the PEDF gene and expression of pigment epithelium-derived factor (PEDF) from the multigenic LV vectors was assessed by immunostaining (Figure 5a) and by western blotting (Figure 5b) of HUVECs transduced with LV/CMV-intron-PEDF-PE. eGFP was broadly distributed in analyzed cells (Figure 5a, upper), whereas PEDF immunostaining indicated localization in the endoplasmic reticulum near the nucleus and in secretory vesicles travelling towards the edge of the cell, as expected for a secretory protein (Figure 5a, lower). PEDF immunostaining of a negatively anti-PEDF stained HUVEC served as a negative control (upper left corner in panels in Figure 5a). The lack of PEDF expression in this cell reflected that not all cells were transduced under the experimental conditions used.

PEDF expression from our LV construct was supported by western blotting revealing an immunoreactive band of ~50 kDa, representing PEDF protein, from both cell lysate and medium from HUVECs transduced with LV/CMV-intron-PEDF-PE. As expected, protein expression increased with increasing amounts of p24, although the amount of secreted protein seemed to reach a saturation point when HUVECs were transduced with more than 100 ng p24.

The functionality of PEDF was assessed by measuring the amount of thrombospondin-1 (TSP-1) mRNA, which is regulated by PEDF in HUVECs, and by investigating the angiogenic potential of LV/CMV-intron-PEDF-PE-transduced HUVECs. As expected, the amount of PEDF mRNA increased in HUVECs, when cells were transduced with increasing amounts of p24 LV (Figure 5c, upper). TSP-1 mRNA levels were found to be significantly increased in HUVECs transduced

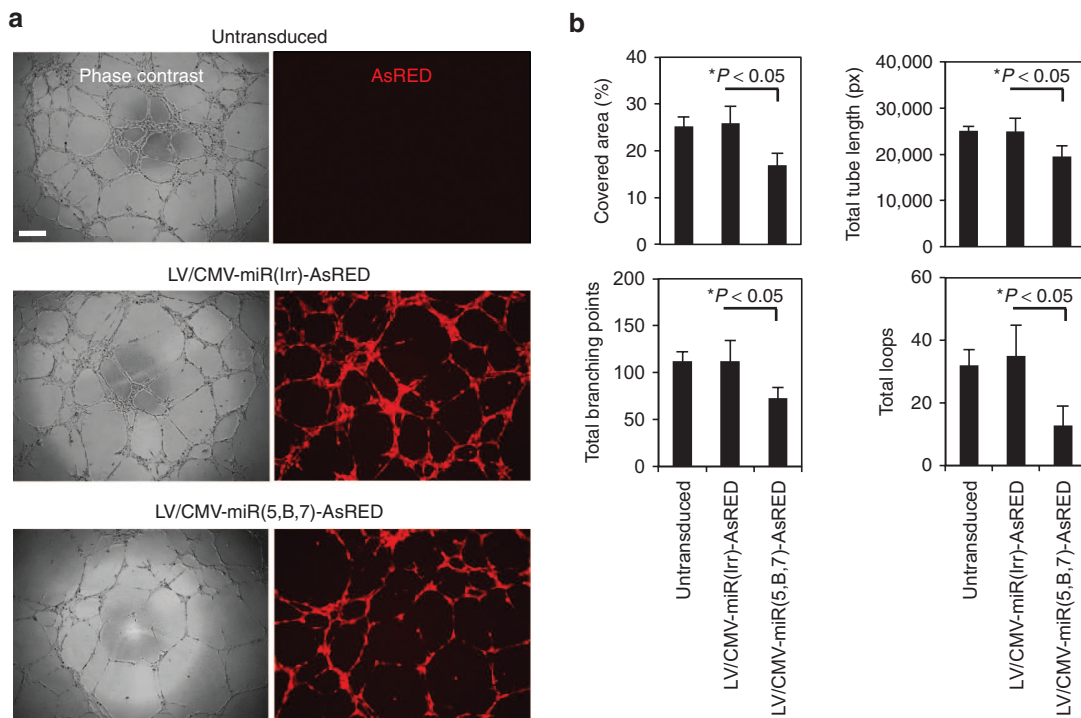


**Figure 4** Inhibition of tube formation in LV/CMV-miR(5,B,7)-AsRED transduced HUVECs.  $1 \times 10^5$  HUVECs were transduced with 100 ng p24 LVs corresponding to a MOI of 3. (a) Representative phase contrast and red fluorescence (AsRED) images of tube formation of untransduced HUVECs (upper panel) and LV/CMV-miR(Irr)-AsRED (mid panel) and LV/CMV-miR(5,B,7)-AsRED (lower panel) transduced HUVECs. Scale bar = 200  $\mu$ m (b) Quantitative analysis of tube formation (mean  $\pm$  SD). \*Statistically significant.

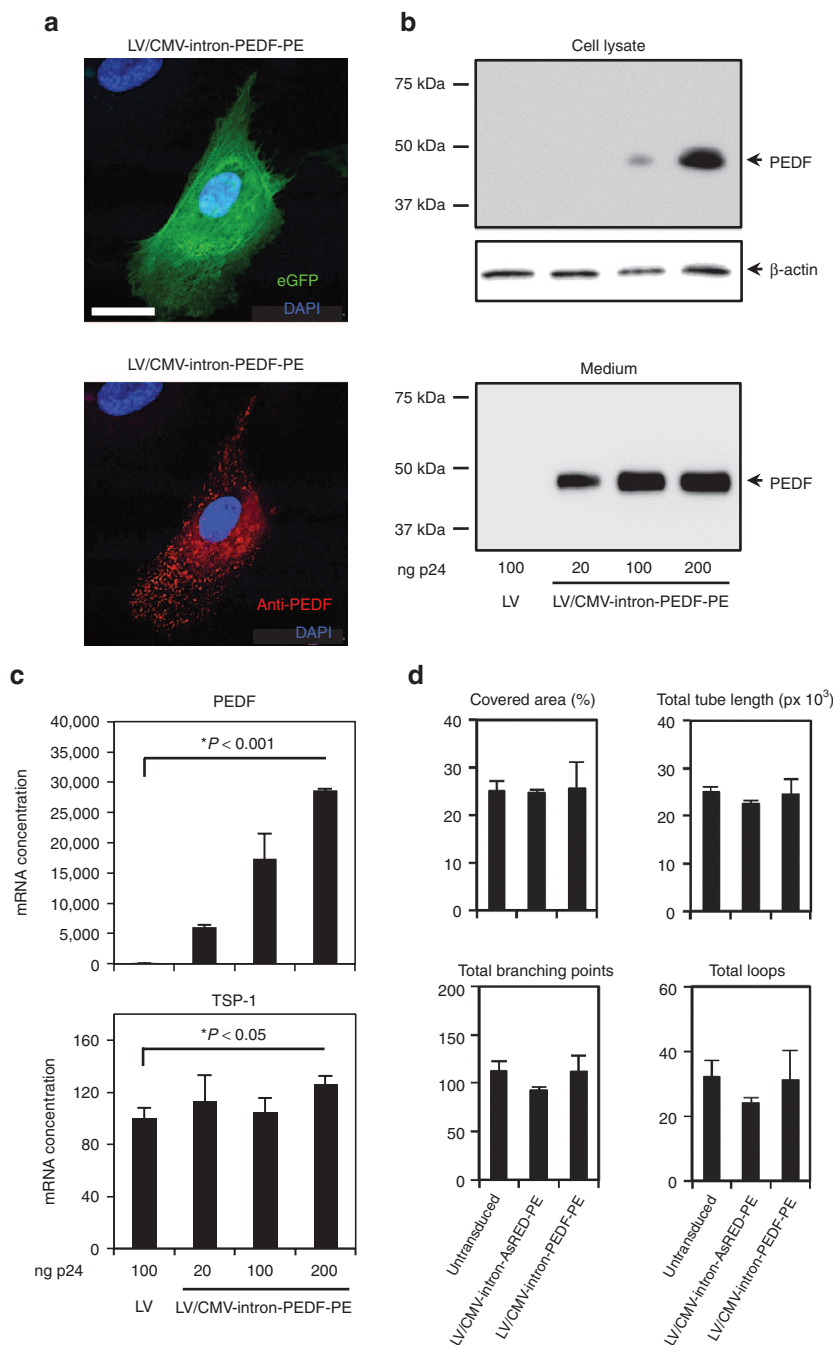


**Figure 5** Expression of PEDF from the multifunction LV vectors in HUVECs. **(a)** Immunostaining of a HUVEC expressing PEDF after LV/CMV-intron-PEDF-PE transduction (100 ng p24 corresponding to a MOI of 3). Staining of the nucleus is shown in blue (DAPI), eGFP expression in green (upper), and anti-PEDF in red (lower). In the upper left corner, a negative anti-PEDF-stained control cell is shown. Scale bar = 20  $\mu$ m. **(b)** Western blot analysis of 15  $\mu$ g total protein extract (upper) and 24  $\mu$ l medium (lower) from HUVECs transduced with 20, 100, or 200 ng p24 of LV/CMV-intron-PEDF-PE, corresponding to MOIs of 0.6, 3, and 6, respectively. The negative control (LV) is HUVECs transduced with 100 ng p24 LV/CMV-intron-AsRED-PE, corresponding to a MOI of 3. The cell lysate and medium fractions were subjected to electrophoresis, blotting and immunostaining using a mouse anti-PEDF antibody. As a loading control for the cell lysate samples, a rabbit antibody against  $\beta$ -actin was used. The positions of PEDF and  $\beta$ -actin are indicated on the right. **(c)** RNA harvested from HUVECs transduced with 20, 100, or 200 ng p24 of LV/CMV-intron-PEDF-PE (corresponding to MOIs of 0.6, 3 and 6, respectively) or with 100 ng p24 LV/CMV-intron-AsRED-PE (corresponding to a MOI of 3) was subjected to quantitative RT-PCR using PEDF, TSP-1, and HPRT primers. The PEDF (upper) and TSP-1 (lower) mRNA concentrations in the LV/CMV-intron-PEDF-PE transduced HUVECs are normalized to the HPRT mRNA concentration and presented relative to LV/CMV-intron-AsRED-PE transduced HUVECs (mean  $\pm$  SD). **(d)** The angiogenic potential of LV/CMV-intron-PEDF-PE transduced HUVECs was not found to be significantly reduced compared to LV/CMV-intron-AsRED-PE transduced HUVECs. Quantitative analysis of cell covered area, total tube length, total number of branching points and loops are shown (mean  $\pm$  SD). The values for the LV/CMV-intron-PEDF-PE transduced HUVECs were not significantly different from the other groups. \*Statistically significant. HPRT, Hypoxanthine-guanine phosphoribosyl transferase; PEDF, pigment epithelium-derived factor; TSP-1, Thrombospondin-1.

with 200 ng LV/CMV-intron-PEDF-PE 6 days after transduction compared to control cells transduced with LV/CMV-intron-AsRED-PE (Figure 5c, lower). However, the angiogenic potential was not found to be significantly reduced in HUVECs transduced with 100 ng LV/CMV-intron-PEDF-PE compared to HUVECs transduced with LV/CMV-intron-AsRED-PE (Figure 5d). This finding suggested that the amount of PEDF expressed from the transduced cells was not high enough to have an effect on tube formation in this assay set-up.

These results demonstrate efficient expression and functionality of PEDF from the multigenic LV vectors and, moreover, regulation of the amount of expressed PEDF by adjusting the levels of p24.

To verify parallel expression of miRNAs and PEDF codelivered by the multigenic LV particle, HEK-293 cells were transduced with LV/CMV-miR(5,B,7)-PEDF-PE or LV/CMV-miR(Irr)-PEDF-PE. The transduction efficiency was inspected by fluorescence microscopy and revealed, as expected, strong AsRED expression in the majority of the cells (data not shown). Four days after transduction, cells were divided in two groups. Cells from one group was immediately fixated and the PEDF expression was analyzed by means of immunostaining. In the other group, the cells were transfected with the psiCHECK-mVEGF reporter, and VEGF silencing was assessed by measuring RLuc/PLuc activity in cell extracts. As shown in Figure 6, transduction with LV/CMV-miR(5,B,7)-PEDF-PE vector resulted in robust miRNA-directed downregulation of VEGF expression and, in parallel, overexpression of

PEDF. The LV/CMV-miR(5,B,7)-PEDF-PE vector was able to downregulate the mVEGF reporter by ~40% compared to the LV/CMV-intron-PEDF-PE vector ( $*P < 0.0035$ ) (Figure 6a). This is almost identical to the data obtained by using the LV/CMV-miR(5,B,7)-AsRED, supporting the notion that insertion of PEDF instead of AsRED does not change the titer (see Figure 3b). As shown in Figure 6b, immunostaining analysis of cells transduced with LV/CMV-miR(5,B,7)-PEDF-PE revealed expression of PEDF protein with an apparent localization in the endoplasmic reticulum near the nucleus as well as in secretory vesicles, which is similar to the staining pattern observed in transduced HUVECs (see Figure 5a). In summary, the multigenic lentiviral vectors demonstrate robust miRNA-directed downregulation of VEGF expression, leading to reduced angiogenesis, and parallel impairment of angiogenic pathways by codelivering PEDF.

## DISCUSSION

Our results show functionality and efficacy of complex LV vectors with potential applicability in the development of an alternative combinational treatment for retinal neovascular diseases. This is supported by our results showing (i) lentiviral titers sufficient for *in vivo* applications of complex constructs despite multiple gene cassettes and volume limitations, as demonstrated by eGFP and AsRED coexpression in mouse retina following subretinal delivery, (ii) significant downregulation of VEGF expression as well as inhibition of VEGF-mediated tube formation *in vitro* by LV-mediated expression of multiple anti-VEGF miRNAs, (iii) coexpression of multiple miRNAs with therapeutic proteins, such as the multifunctional protein PEDF from the multigenic vector, and (iv) targeted transcription of a single mRNA, encoding miRNAs and protein from the LV construct, in retinal target cells such as the RPE cells by incorporation of a tissue-specific promoter.

Current treatment options for patients suffering from exudative AMD, including anti-VEGF and photodynamic therapy, all have in common that repeated treatments are necessary; for some of the treatments, monthly therapy is required. Patients as well as the health care system are struggling with the burden that comes with the need of monthly care involving an invasive therapy that for most patients will require a lifetime of treatment. Additionally, some patients do not benefit from established treatments. Fortunately, several new therapies are appearing, some of which have the potential to once more, noticeably change the treatment modality for AMD patients. These modalities revolve around gene therapy, with proof of concept for ocular gene therapy established with treatment of Leber congenital amaurosis.<sup>16-18</sup> At present, several gene therapy-based treatments are being evaluated in clinical trials. Most of them include expression of an antiangiogenic protein from viral vectors: PEDF from adenovirus,<sup>19</sup> soluble VEGF receptors (sFlt-1 (ref. 20) or sFLT01 (ref. 21)) from AAV or Endostatin and Angiostatin from an LV vector.<sup>22</sup> A few have involved delivery of synthetic siRNAs, but two out of three unfortunately failed to meet the efficacy requirements.

In this study, we have designed and evaluated multigenic LV vectors with combined expression of multiple anti-VEGF miRNAs and proteins. With the miRNA-based delivery approach, it is possible to simultaneously target (i) multiple regions in a single mRNA or (ii) several different genes, thereby providing a broader applicability allowing fine-tuned expression and enhanced cellular processing. This approach has been applied for knocking down three different genes from a single lentiviral vector.<sup>23</sup> In addition, we have in a previous study shown effectfull miRNA-mediated knockdown of VEGF from a single AAV vector expressing three different anti-VEGF siRNAs.<sup>12</sup> We believe LV-delivered anti-VEGF miRNAs have

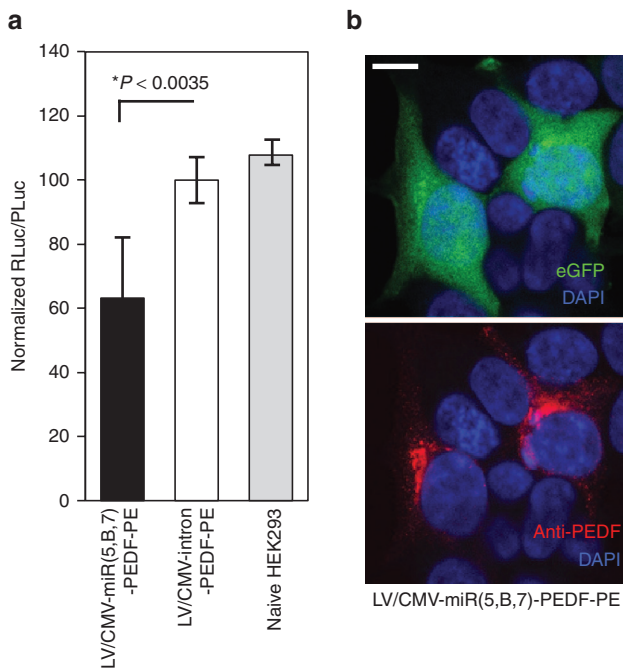


**Figure 6** Simultaneous expression of miRNAs and PEDF from the multigenic LV/CMV-miR(5,B,7)-PEDF-PE vectors in HEK-293 cells. Crude LV/CMV-miR(5,B,7)-PEDF-PE or LV/CMV-intron-PEDF-PE was added to  $1 \times 10^6$  HEK-293 cells corresponding to a MOI of ~2.5. (a) miRNA-mediated RLuc-VEGF knockdown 6 days after transduction in LV/CMV-miR(5,B,7)-PEDF-PE, or LV/CMV-intron-PEDF-PE treated HEK-293 cells demonstrated by using the dual luciferase assay. Nontransduced (naïve) HEK-293 cells were used as negative control. Expression of *Renilla* luciferase activity (RLuc) was normalized to the expression of the internal *P. photinus* luciferase (PLuc) as a transfection control and values are presented relative to levels in cells transduced with LV/CMV-intron-PEDF-PE (mean  $\pm$  SD). \*Statistically significant. (b) Immunostaining of HEK-293 cells expressing PEDF after LV/CMV-miR(5,B,7)-PEDF-PE transduction. Staining of the nucleus is shown in blue (DAPI), eGFP expression in green (upper), and anti-PEDF in red (lower). Scale bar = 10  $\mu$ m. PLuc, Firefly luciferase; RLuc, *Renilla* luciferase.

significant advantage over synthetic siRNAs in that they are continuously expressed endogenously in target cells following a single injection. Additionally, utilization of miRNA-based delivery strategies overcomes the obstacles encountered with siRNA-based treatments, such as sequence- and target-independent toll-like receptor 3 mediated suppression of angiogenesis,<sup>9</sup> and are less prone to interfere with the endogenous miRNA processing compared to shRNA delivered with strong polymerase III promoters, thus exhibiting an improved safety profile.<sup>24–26</sup> Even though insertion of a second expression cassette (CMV-intron) resulted in 12-fold reduction in the titer, which is similar to previous findings,<sup>27</sup> the bidirectional vectors demonstrated robust miRNA-directed downregulation of VEGF expression and parallel overexpression of PEDF.

After investigating the basic functionality of the multigenic LV vectors, we wanted to ensure that we could obtain titers sufficient for *in vivo* applications. For *in vivo* studies, we included an RPE-specific promoter (VMD2) to limit transgene expression to RPE cells, the cells responsible for overexpression of VEGF in AMD patients.<sup>28</sup> The transduction profile and efficiency of an LV vector incorporating the VMD2 promoter were evaluated in mice following subretinal delivery, and reporter gene expression demonstrated efficient gene transfer limited to RPE cells, as shown previously by other groups.<sup>29,30</sup>

When we combined two or three anti-VEGF miRNAs in the same cluster, we observed in this study an improved VEGF silencing effect compared to our previous studies.<sup>12</sup> We found that substitution of the miRNA in the second position significantly improved the anti-VEGF effect of the miRNA clusters compared to our previous results,<sup>12</sup> where we obtained a reduced VEGF silencing effect when miR(9) or miR(10) was incorporated in mono- or bicistronic constructs. These results indicate that the poor functionality can be rescued by proper design of the miRNA. However, the total VEGF silencing found in this study ( $78 \pm 2\%$  in HEK-293) was comparable to our previous study ( $75 \pm 1\%$  in ARPE-19).<sup>12</sup>

LV-mediated delivery of anti-VEGF miRNAs was able to significantly downregulate VEGF in HEK-293 ( $38 \pm 2\%$ ) and melanoma cells ( $49 \pm 5\%$ ). The difference in VEGF knockdown efficacy of the miR(5, B, 7) in the cotransfected cells compared to the LV-transduced cells, is believed to be due to the different amount of psiCHECK vectors used as well as a difference in the ratio of miRNA to VEGF reporter expression cassettes in the cells. The latter is due not only to differences in study design, but also in cellular uptake of LV-delivered transduction and plasmid-based transfection mechanisms.<sup>31</sup>

We have demonstrated that anti-VEGF miRNAs can inhibit tube formation *in vitro*. HUVECs transduced with the LV/CMV-miR(5, B, 7)-AsRED construct also exhibited red fluorescence, indicating functional expression of both miR(5, B, 7) and AsRED in the HUVECs. Incorporation of reporter genes such as AsRED or eGFP allows easy visualization of transgene expression *in vitro* as well as *in vivo*. Furthermore, miRNA expressing cells can be easily traced by the concomitant AsRED expression.

AsRED was exchanged with PEDF, and expression was confirmed by immunostaining and western blot. Functional expression was verified by qPCR, demonstrating increased amounts of TSP-1 mRNA, an endogenous angiogenic inhibitor that inhibits proliferation of endothelial cells, in HUVECs transduced with 200 ng p24 of LV/CMV-intron-PEDF-PE, which is in accordance with previous findings.<sup>32</sup> We could not demonstrate an antiangiogenic effect in the tube forming assay. Others have been able to show inhibition of VEGF-mediated angiogenesis in the tube forming assay,<sup>33,34</sup> and shown that addition of recombinant PEDF can inhibit tube formation in this assay.<sup>35</sup> We believe that our finding can be due

to sub-optimal assay conditions including insufficient amounts of PEDF. In this assay, HUVECs were transduced with 100 ng of p24, which is likely to be insufficient for PEDF to have an effect. A delayed effect of secreted PEDF from the transduced HUVECs was precluded by inspection after 24 hours also and by utilization of conditioned medium (data not shown).

Based on our data, a combination therapy of LV-delivered antiangiogenic miRNAs and protein for treatment of intraocular neovascular diseases may be proposed. Efficient coexpression of miRNAs and two proteins from a single viral vector may minimize the viral load necessary to obtain a therapeutic effect and thereby reduce the risk of insertional mutagenesis as well as the immune response against viral proteins. Furthermore, the subretinal delivery strategy has volume limitations underscoring the applicability of efficient, multigenic viral vectors for retinal gene transfer. For immunotherapy for cancer patients, Okamoto *et al.* have developed murine leukemia virus-based vectors encoding siRNAs to knockdown endogenous T-cell receptor (TCR) genes and a therapeutic siRNA-resistant tumor antigen-specific TCR simultaneously.<sup>36</sup> The LV vectors were chosen in the present study due to their ability to transduce nondividing cells and in contrast to the AAV vectors, they have a large packaging capacity, required for packing of the multigenic and PE expression cassettes. Presently there is a rapidly growing interest in the LV vectors for ocular gene therapy, and three LV-based clinical trials are currently open (clinicaltrials.gov). Concerns regarding insertional mutagenesis can be further reduced by utilizing integrase-defective LV vectors.<sup>37</sup>

In conclusion, our results show expression of therapeutic anti-VEGF-miRNAs and PEDF from a single cassette and efficient gene transfer to mouse retinal cells when delivered by the versatile LV vector, demonstrating the potential applicability of multigenic LV vectors in ocular anti-VEGF gene therapy, including combination therapy for treatment of exudative AMD.

## MATERIALS AND METHODS

### Cell culture, transfection, and transduction

Five different cell lines were used in this study. A human adult retinal pigment epithelial cell line (ARPE-19; catalog number CRL-2302; American Type Culture Collection, Boras, Sweden) was maintained in Dulbecco's modified Eagle's medium (DMEM)/F12 Nutrient Mixture;1:1 (Gibco, Invitrogen, Taastrup, Denmark) with 10% fetal calf serum (Sigma-Aldrich, Broendby, Denmark), 0.06 mg/ml penicillin (FarmaPlus, Oslo, Norway), 0.1 mg/ml streptomycin and 0.29 mg/ml glutamine (both Sigma-Aldrich). HEK-293 cells (catalog number CRL-1573; American Type Culture Collection), HEK-293T cells,<sup>38</sup> and melanoma cells<sup>13</sup> were maintained in DMEM (Gibco; Invitrogen) containing 0.29 mg/ml glutamine (Sigma-Aldrich), 0.06 mg/ml penicillin (Farma-Plus) and 0.1 mg/ml streptomycin (Sigma-Aldrich) and supplemented with 10% fetal calf serum (Sigma-Aldrich). Human umbilical vein endothelial cells (HUVECs; catalog number CC-2517, Lonza, Basel, Switzerland) were maintained in endothelial cell growth medium 2 (EGM2) (BioNordika, Herlev, Denmark) supplemented with 0.06 mg/ml penicillin (Farma-Plus) and 0.1 mg/ml streptomycin (Sigma-Aldrich) and for the tube forming assay, endothelial cell growth medium (EGM) (BioNordika) supplemented with 0.06 mg/ml penicillin (Farma-Plus) and 0.1 mg/ml streptomycin (Sigma-Aldrich) was used.

Cells were cultivated in tissue culture flasks or plates (TPP Techno Plastic Products AG, Trasadingen, Switzerland) at 37 °C with 5% (v/v) CO<sub>2</sub> as described previously.<sup>39</sup> All transfection experiments were carried out in triplicates or five copies at 25% confluency using X-tremeGENE 9 (Roche Applied Science, Hvidovre, Denmark) for transfection of HEK-293 cells (ratio DNA:transfection reagent 1:4) and JetPrime transfection reagent for transfection of melanoma cells (ratio DNA:transfection reagent 1:2).

Before transduction of HEK293, ARPE-19, and HUVECs the culture medium was removed and replaced with fresh culture medium containing 8 µg/ml polybrene (Sigma-Aldrich). For transduction of melanoma cells, no polybrene was used.



## Vector construction

The design of the miRNAs has been described in our previous study.<sup>12</sup> In this study, we modified miR(5) and miR(7)<sup>12</sup> to target murine VEGF<sub>164</sub>, and miR(B) was adapted from a previous study<sup>4</sup> and modified to target murine VEGF<sub>164</sub>. miR(5), miR(B), and miR(7) were designed to perfectly match the mouse ortholog. The different miRNAs directed against mVEGF were inserted in the optimized miR-106b cluster driven by the cytomegalovirus (CMV) promoter (pCDNA3.1-based plasmid, designated pCM in this study)<sup>15</sup> by independent replacement of each of the three anti-HIV miRNAs. Inserts were generated by PCR extension of partially annealed overlapping ~60-nucleotide oligonucleotides (Eurofins MWG Operon, Ebersberg, Germany), followed by digestion with the appropriate restriction enzymes. Thus, in total, seven different clusters comprised of heterologous hairpin entities were generated by permutational insertions into the S1, S2, and S3 positions as *XhoI/HindIII*, *EcoRI/BamHI* or *XbaI/SacI* fragments, respectively. The resulting plasmids were named pmiR(x,y,z) (x,y,z being the order of the different anti-VEGF miRNAs). The anti-HIV miR-S1,S2,S3 cluster was used as an irrelevant control (referred to as miR(Irr)).

The multigenic LV vectors were generated by replacing the EF1 $\alpha$  promoter in pLV/EF1 $\alpha$ -intron-PE (PE denotes the PGK-eGFP expression cassette) with the CMV or the VMD2 promoter (L. Aagaard, unpublished). The CMV promoter was amplified from the pCM plasmid by PCR using Herculase II fusion DNA polymerase (Agilent Technologies, AH Diagnostics, Aarhus, Denmark) and CMV specific-primers harboring *MluI* and *Sall* restriction enzyme recognition sequences followed by digestion with *MluI* and *Sall*. Following *MluI* and *Sall* double digestion, the CMV sequence was inserted in the linearized pLV/EF1 $\alpha$ -intron-PE plasmid replacing EF1 $\alpha$ . The resulting vector was named pLV/CMV-intron-PE. The VMD2 promoter sequence was obtained from a previous study.<sup>29</sup> The -585 to +38 bp sequence upstream of human *VMD2* gene was synthesized by GenScript (Piscataway, NJ) flanked by *MluI* and *Sall* restriction sites. Following *MluI* and *Sall* double digestion, the VMD2 sequence was inserted in the linearized pLV/EF1 $\alpha$ -intron-PE plasmid replacing EF1 $\alpha$ . The resulting vector was named pLV/VMD2-intron-PE. The bovine growth hormone polyA site is utilized as termination sequence in the CMV/VMD2 expression cassette, whereas expression from the PE cassette is terminated by the viral 3'LTR.

The constructs without the PE expression cassette are generated by removing PE by *MluI* and *XhoI* double digest followed by T4 DNA polymerase (New England Biolabs, Ipswich, MA) reaction to generate blunt ends and subsequently, the plasmid was religated.

AsRED was amplified from the pAAV2-siRNA vector (catalog number 0914; Applied Viromics, Fremont, CA) by PCR using Herculase II fusion DNA polymerase (Agilent Technologies) and AsRED specific-primers harboring the *XmaI* restriction enzyme recognition sequence. Following *XmaI* digestion, the AsRED sequence was inserted in the linearized pLV/CMV-intron-PE or pLV/VMD2-intron-PE plasmid. The resulting vectors were named pLV/CMV-intron-AsRED-PE and pLV/VMD2-intron-AsRED-PE, respectively.

PEDF was acquired from Source BioScience (Cambridge, UK) as an Image cDNA clone (IMAGE ID 235156). PEDF was amplified from the vector harboring the Image Clone by PCR using Herculase II fusion DNA polymerase (Agilent Technologies) and PEDF specific-primers harboring the *XmaI* restriction enzyme recognition sequence. Following *XmaI* digestion, the PEDF sequence was inserted in the linearized pLV/CMV-intron-PE or pLV/CMV-intron-AsRED-PE plasmids. The resulting vectors were named pLV/CMV-intron-PEDF-PE and pLV/CMV-intron-AsRED-PEDF, respectively.

The anti-VEGF miRNA miR(5,B,7) and irrelevant miR(Irr) clusters were amplified from the pCM/miR(5,B,7) and pCM/miR(Irr), respectively, by PCR using OneTaq DNA polymerase (New England Biolabs, Ipswich, MA) and primers harboring the *BsiWI* and *NsiI* restriction enzyme recognition sequences. Following *BsiWI* and *NsiI* double digestion, the miR(Irr) or miR(5,B,7) cluster sequences were inserted in the linearized pLV/CMV-intron-AsRED, pLV/CMV-intron-AsRED-PE, pLV/CMV-intron-PEDF-PE, pLV/VMD2-intron-AsRED, and pLV/VMD2-intron-AsRED-PE plasmids. The resulting vectors were named pLV/CMV-miR(Irr)-AsRED, pLV/CMV-miR(5,B,7)-AsRED, pLV/CMV-miR(5,B,7)-AsRED-PE, pLV/CMV-miR(5,B,7)-PEDF-PE, pLV/VMD2-miR(Irr)-AsRED, pLV/VMD2-miR(5,B,7)-AsRED, and pLV/VMD2-miR(5,B,7)-AsRED-PE, respectively.

For generation of a dual luciferase reporter construct to serve as a platform for testing the anti-VEGF miRNA clusters, the psiCHECK-mVEGF plasmid was produced. Changes in expression of the *Renilla* luciferase reporter gene fused to the mVEGF gene were used as an indicator of the efficacy of the anti-VEGF miRNAs. The mVEGF<sub>164</sub> cDNA sequence (GenBank accession number BC061468.1) was synthesized by GenScript flanked by *NotI* and *XhoI* restriction sites and cloned into unique *NotI* and *XhoI* sites in the 3'-UTR of the *Renilla* luciferase gene of the psiCHECK-2 Vector (Promega, Stockholm, Sweden).

Plasmid DNA was purified using Plasmid Plus kits (Qiagen Nordic, Copenhagen, Denmark). All constructs were verified by restriction analysis and sequencing. Primer sequences are available upon request.

## LV production, purification, and titer assessment

For cell studies, crude LV preparations (preps) were made and for subretinal injections, the LV preps were concentrated by ultracentrifugation. On day 1.1  $\times 10^7$  (or 4  $\times 10^6$ ) HEK-293T cells were seeded in a p15 (or a p10) dish. On day 2, cells were transfected with calcium phosphate precipitates. Each of the p15 dishes were transfected with 9.1  $\mu$ g pMD.2G, 7.3  $\mu$ g pRSV-Rev, 31.5  $\mu$ g pMDLg/pRRE, and 31.5  $\mu$ g pLV. The p10 dishes were transfected with 3.75  $\mu$ g pMD.2G, 3  $\mu$ g pRSV-Rev, 13  $\mu$ g pMDLg/pRRE, and 13  $\mu$ g pLV. The medium was replaced on day 3. On day 4, viral supernatants were harvested, and passed through a 0.45  $\mu$ m filter (Millipore A/S, Hellerup, Denmark). LV particles produced for subretinal injections were further purified and concentrated by ultracentrifugation through a sucrose cushion at 25,000 rpm for 2 hours in a SW28 rotor (Beckman Coulter, Fullerton, CA). Pellets were resuspended in phosphate-buffered saline (PBS) and stored at -80  $^{\circ}$ C.

Concentrations of HIV-1 p24 were measured by enzyme-linked immunosorbent assay (ZeptoMetrix, Buffalo, NY) according to the manufacturer's protocol. Number of transducing units per ml (TU/ml) was determined by flow cytometry. On day 1, 10<sup>5</sup> HEK-293 cells were seeded in six-well plates. On day 2, cells were transduced with crude virus with dilutions of 0.5, 10<sup>-1</sup>, and 10<sup>-2</sup>. On day 3, the medium containing virus was removed and replaced with 2 ml of fresh culture medium. On day 7, the cells were collected and washed in PBS before fixation in neutral buffered formalin (NBF). Flow analysis was performed to record the percentage of cells that were GFP and AsRED double positive compared to the negative control cells. For cells only expressing AsRED or GFP, the percentage of AsRED positive or GFP positive cells were used, respectively. Data were collected on a 4-laser LSRFortessa (BD Biosciences, San Jose, CA) and analyzed with FlowJo (Tree Star, Ashland, OR). A well that had between 1 and 20% of cells expressing GFP and/or AsRED was used to determine lentiviral titer by the formula: TU/ml = ((F  $\times$  C<sub>n</sub>)/V)  $\times$  DF, where F is the frequency of GFP and/or AsRED-positive cells determined by flow cytometry; C<sub>n</sub> is the total number of target cells infected; V is the volume of the transducing inoculum in ml and DF is the virus dilution factor. For each individual experiment, the estimated virus dose per cell (MOI) was based on the correlation that 1 pg HIV-1 p24 unit corresponds to 3 TU as determined in HEK293 cells transduced with LV/CMV-intron-AsRED-PE.

## Dual-luciferase assay

A dual luciferase reporter construct, psiCHECK-mVEGF, was generated as described previously<sup>11</sup> to serve as a platform for testing the efficacy of the anti-VEGF miRNAs. To test the efficacy of the seven different anti-VEGF miRNA clusters, 2  $\times 10^4$  HEK-293 cells were seeded in 24-well plates. The following day, cells were transfected with 40 ng psiCHECK-mVEGF plasmid and 360 ng of the indicated plasmid harboring one of the seven different miRNA clusters per well (triplicates). Forty-eight hours after transfection, cells were lysed and luciferase levels analyzed using the Dual-Luciferase Reporter Assay System (Promega). To test the efficacy of miRNA clusters delivered by LV particles, 2  $\times 10^5$  HEK-293 and melanoma cells in six-well plates were transduced with 100 ng p24 LV/CMV-miR(5,B,7)-AsRED, LV/CMV-miR(Irr)-AsRED, LV/CMV-miR(5,B,7)-PEDF-PE, LV/CMV-intron-PEDF-PE or LV/VMD2-miR(5,B,7)-AsRED and LV/VMD2-miR(Irr)-AsRED particles, respectively. Four days after transduction, 3  $\times 10^5$  LV transduced HEK-293 or melanoma cells were seeded in 96-well plates (n = 5). The following day, cells were transfected with 48 or 96 ng psiCHECK-mVEGF plasmid and 48 hours after transfection, cells were lysed and luciferase levels analyzed using the Dual-Glo Luciferase Assay System (Promega). Changes in the expression of *Renilla* luciferase (RLuc) were normalized to *Photinus pyralis* luciferase (PLuc) and presented relative to levels in cells transduced with miR(Irr).

## RNA isolation, cDNA synthesis, and PCR analysis

RNA was extracted from LV/CMV-intron-AsRED-PE transduced HEK-293 cells 48 hours after transduction using RNeasy Mini Kit and DNase treatment according to the manufacturer's instructions (Qiagen Nordic). cDNA was generated by reverse transcription of 0.5  $\mu$ g RNA using oligo (dT), random hexamer primers, and iScript cDNA Synthesis Kit (Bio-Rad Laboratories, Hercules, CA). A standard PCR amplification was performed using ~10 ng cDNA or plasmid DNA as template and primers annealing in the 5' exon sequence and the AsRED sequence amplifying a large 1,270 bp fragment if no splicing occurs, and a small 791 bp fragment if splicing occurs.

The resulting PCR fragments were subjected to agarose gel electrophoresis. All primer sequences and PCR conditions are available upon request. RT-PCR was performed as previously described.<sup>11</sup>

### miRNA purification and northern blot analysis

HEK-293 cells were transfected in culture flasks (surface area 75 cm<sup>2</sup>) at 25% confluency using X-tremeGENE 9 (Roche Applied Science). Total RNA was isolated 48 hours after transfection using the mirVana miRNA Isolation Kit (Ambion, Austin, TX). For detection of miRNA expression, 20 µg of total RNA was electrophoresed in 10% denaturing polyacrylamide gel electrophoresis (Criterion Precast gel 10% TBE-urea (BioRad, Copenhagen, Denmark)) in 1x TBE buffer for 30 minutes at 200V together with a RNA size marker (decade marker RNA; Ambion). The RNA was transferred to a positively charged nitrocellulose membrane, Amersham Hybond-N (GE Healthcare, Little Chalfont, UK) by electroblotting (Trans-blot SD semi-dry transfer cell; BioRad). Ultraviolet-fixed membranes were hybridized overnight in PerfectHyb solution (Sigma-Aldrich, St Louis, MA) at 42 °C with purified 5' <sup>32</sup>P-labeled oligos complementary to the predicted mature miRNA strand. The oligo probes (10 pmol) were end-labeled with PNK (10 units; NEB) and γ<sup>32</sup>P-ATP (10 µCi) in 10 µl reactions for 1 hour, and purified with G-25 Sephadex spin-columns (GE Healthcare). Hybridized membranes were washed twice with 6 × SSC/0.2% SDS, and then twice with 2 × SSC/0.1% SDS, before exposure to film (CL-XPosureTM Film, Rockford, IL). Probe 5: 5'-GGATGCTACCAGCGAAGCTA-3, probe B: 5'-AAACCTCACCAAAGCCAGCAC, probe 7: AGACAGAACAAAGCCAGAAAA, U6 small nuclear RNA(snRNA)-specific probe: 5'-TATGGAACGCTTCTCGAATT-3.

### Western blot analysis

HUVECs were transfected in six-well plate at 25% confluency with 20, 100, or 200 ng p24 LV/CMV-intron-PEDF-PE or 100 ng p24 LV/CMV-intron-AsRED-PE as negative control, and subsequently subcultured in T25 flasks. Harvest, lysis and western blotting were performed as described previously.<sup>40</sup> In short, cells were lysed 5 days after transduction in 100 µl of lysis buffer. 15 µg of total protein or 24 µl medium were electrophoresed on a 12% polyacrylamide gel (Mini-PROTEAN TGX gels; BioRad) together with the Precision Plus Protein Standard marker (BioRad). Following transfer to a Trans-Blot Turbo PVDF Membrane (Bio-Rad Laboratories), PEDF was detected using monoclonal mouse antipeptide epithelium-derived factor antibody (MAB1059; Millipore). As a loading control, rabbit polyclonal antibody against β-actin (Abcam 8227-50; Abcam, Cambridge, MA) was used. Detection was performed using secondary horseradish peroxidase-conjugated polyclonal goat antimouse and polyclonal goat antirabbit antibodies, respectively (numbers P0447 and P0448; Dako, Glostrup, Denmark). Bound antibodies were visualized with SuperSignal West Dura Extended Duration Substrate (Thermo Scientific, Waltham, MA) on an ImageQuant LAS4000 digital imaging system (GE Healthcare, Cleveland, OH).

### Immunostaining

HUVECs were transfected in six-well plates at 25% confluency with 100 ng p24 LV/CMV-intron-PEDF-PE or LV/CMV-intron-AsRED-PE and subsequently subcultured in slide flasks. Approximately 1 × 10<sup>6</sup> HEK-293 cells were transfected in p10 dishes with 5 ml LV/CMV-miR(5,8,7)-PEDF-PE. Five days after transduction, the cells were fixed in 4% paraformaldehyde (Hounisen, Risskov, Denmark) and stained with mouse monoclonal PEDF antibody (Millipore MAB1059) as described previously.<sup>39</sup> Detection was performed using secondary Alexa Fluor 568 goat antimouse antibody (catalog number A11004; Invitrogen). Nuclei were stained with 4',6-diamidino-2-phenylindole (Sigma-Aldrich). Cells were visualized using a confocal laser scanning microscope (LSM 710, Zeiss, Jena, Germany).

### Tube forming assay

Day 1, 1 × 10<sup>5</sup> HUVECs were seeded in six-well plates and transfected with 100 ng p24 LV/CMV-miR(Irr)-AsRED or LV/CMV-miR(5,8,7)-AsRED the following day. Day 5, the cells were subcultured in T25 flask. Day 7, the culture medium was changed from EGM-2 to EGM (without VEGF). Day 8, 1 × 10<sup>4</sup> cells were seeded onto 10 µl BD matrigel (Basement Membrane Matrix, Growth Factor Reduced) (BD Biosciences) in a 15-well µ-Slide Angiogenesis ibiTreat (Ibidi GmbH, Planegg/Martinsried, Germany) in EGM medium. After 4 hours, tube formation was inspected by fluorescence microscopy (Leica DM IRBE) and images captured with a Leica DFC 320 camera. One photo was taken in the center of the well. Cell covered area, tube length, total number of branching points and loops was quantified with WimTube image analysis (Ibidi).

In the tube forming assay performed with LV/CMV-intron-AsRED-PE and LV/CMV-intron-PEDF-PE transduced HUVECS, cells were seeded in the conditioned EGM medium that was removed from the cells before harvest on day 8.

### Animals

For the ocular injections, C57BL/6J mice were purchased from Charles River (Arbresle, France) and maintained under a 12:12 hours light/dark cycle. The animals were handled in accordance with the statement of the "Animals in Research Committee" of the Association for Research in Vision and Ophthalmology, and protocols were approved by the local Swiss institutional committee, the "Service de la consommation et des affaires vétérinaires du canton de Vaud" (authorization VD#1367.3).

### Subretinal LV injections

Subretinal injections were performed as described previously.<sup>11</sup> The final dose of LV/VMD2-miR(5,8,7)-AsRED-PE (two mice, bilateral injections) was 30 ng p24 per eye in a total volume of 2 µl.

### Cryosectioning and histological analysis

Twenty-one days after the subretinal injection, eyes were enucleated, fixed, and cut as previously described.

For histological analysis, the 7-µm sections were thawed and rehydrated with PBS + 1% TritonX-100. Nuclei were stained with 4',6-diamidino-2-phenylindole (Sigma-Aldrich) and after washing with PBS, the sections were mounted in Mowiol (Sigma-Aldrich). Sections were analyzed for eGFP and AsRED expression by fluorescence microscopy (Leitz DM RB; Leica Microsystems GmbH, Wetzlar, Germany) and images captured with a Leica DFC 360 FX camera and associated software (Leica Application Suite, version 3).

### Statistical analysis

Data are presented as the mean ± SD. Statistical differences between two groups were evaluated using Student's *t*-test and statistical differences between more than two groups were evaluated by linear regression analysis. *P* < 0.05 was considered statistically significant.

### CONFLICT OF INTEREST

The authors declare no conflict of interest.

### ACKNOWLEDGMENTS

We thank Catherine Martin (UGTSCB) for her excellent technical assistance. Flow cytometry was performed at the FACS Core Facility, The Faculty of Health Sciences, Aarhus University, Denmark. This work was supported by the Lundbeck Foundation (Grant No. R44-A4289), Gene Therapy Initiative Aarhus (GTI-Aarhus) funded by the Lundbeck Foundation (Grant No. R126-2012-12456), The Danish Eye Foundation, Aase og Ejnar Danielsens Fond, Civilingeniør Lars Andersens Fond, Augustinus Fonden, Synoptik Fonden, Riisfort Fonden, and the Provisu Foundation. A.L.A. is the recipient of a mobility PhD fellowship from HEALTH, Aarhus University.

### REFERENCES

- Tozer, K, Roller, AB, Chong, LP, Sadda, S, Folk, JC, Mahajan, VB *et al.* (2013). Combination therapy for neovascular age-related macular degeneration refractory to anti-vascular endothelial growth factor agents. *Ophthalmology* **120**: 2029–2034.
- Singerman, L (2009). Combination therapy using the small interfering RNA bevasiranib. *Retina (Philadelphia, Pa)* **29**(6 Suppl): S49–S50.
- Augustin, AJ, Puls, S and Offermann, I (2007). Triple therapy for choroidal neovascularization due to age-related macular degeneration: verteporfin PDT, bevacizumab, and dexamethasone. *Retina (Philadelphia, Pa)* **27**: 133–140.
- Reich, SJ, Fosnot, J, Kuroki, A, Tang, W, Yang, X, Maguire, AM *et al.* (2003). Small interfering RNA (siRNA) targeting VEGF effectively inhibits ocular neovascularization in a mouse model. *Mol Vis* **9**: 210–216.
- Kaiser, PK, Symons, RC, Shah, SM, Quinlan, EJ, Tabandeh, H, Do, DV *et al.*; Sirna-027 Study Investigators. (2010). RNAi-based treatment for neovascular age-related macular degeneration by Sirna-027. *Am J Ophthalmol* **150**: 33–39.e2.

6. Nguyen, QD, Schachar, RA, Nduaka, CI, Sperling, M, Basile, AS, Klamerus, KJ *et al.*; PF-04523655 Study Group. (2012). Phase 1 dose-escalation study of a siRNA targeting the RTP801 gene in age-related macular degeneration patients. *Eye (Lond)* **26**: 1099–1105.
7. Garba, AO and Mousa, SA (2010). Bevasiranib for the treatment of wet, age-related macular degeneration. *Ophthalmol Eye Dis* **2**: 75–83.
8. Nguyen, QD, Schachar, RA, Nduaka, CI, Sperling, M, Klamerus, KJ, Chi-Burris, K *et al.*; MONET Clinical Study Group. (2012). Evaluation of the siRNA PF-04523655 versus ranibizumab for the treatment of neovascular age-related macular degeneration (MONET Study). *Ophthalmology* **119**: 1867–1873.
9. Kleinman, ME, Yamada, K, Takeda, A, Chandrasekaran, V, Nozaki, M, Baffi, JZ *et al.* (2008). Sequence- and target-independent angiogenesis suppression by siRNA via TLR3. *Nature* **452**: 591–597.
10. Cashman, SM, Bowman, L, Christofferson, J and Kumar-Singh, R (2006). Inhibition of choroidal neovascularization by adenovirus-mediated delivery of short hairpin RNAs targeting VEGF as a potential therapy for AMD. *Invest Ophthalmol Vis Sci* **47**: 3496–3504.
11. Askou, AL, Pournaras, JA, Pihlmann, M, Svalgaard, JD, Arsenijevic, Y, Kostic, C *et al.* (2012). Reduction of choroidal neovascularization in mice by adeno-associated virus-delivered anti-vascular endothelial growth factor short hairpin RNA. *J Gene Med* **14**: 632–641.
12. Pihlmann, M, Askou, AL, Aagaard, L, Bruun, GH, Svalgaard, JD, Holm-Nielsen, MH *et al.* (2012). Adeno-associated virus-delivered polycistronic microRNA-clusters for knockdown of vascular endothelial growth factor in vivo. *J Gene Med* **14**: 328–338.
13. Corydon, TJ, Haagerup, A, Jensen, TG, Binderup, HG, Petersen, MS, Kaltoft, K *et al.* (2007). A functional CD86 polymorphism associated with asthma and related allergic disorders. *J Med Genet* **44**: 509–515.
14. Masuda, T and Esumi, N (2010). SOX9, through interaction with microphthalmia-associated transcription factor (MITF) and OTX2, regulates BEST1 expression in the retinal pigment epithelium. *J Biol Chem* **285**: 26933–26944.
15. Aagaard, LA, Zhang, J, von Eije, KJ, Li, H, Saetrom, P, Amarzguioui, M *et al.* (2008). Engineering and optimization of the miR-106b cluster for ectopic expression of multiplexed anti-HIV RNAs. *Gene Ther* **15**: 1536–1549.
16. Bainbridge, JW, Smith, AJ, Barker, SS, Robbie, S, Henderson, R, Balaggan, K *et al.* (2008). Effect of gene therapy on visual function in Leber's congenital amaurosis. *N Engl J Med* **358**: 2231–2239.
17. Maguire, AM, Simonelli, F, Pierce, EA, Pugh, EN Jr, Mingozzi, F, Bennicelli, J *et al.* (2008). Safety and efficacy of gene transfer for Leber's congenital amaurosis. *N Engl J Med* **358**: 2240–2248.
18. Hauswirth, WW, Aleman, TS, Kaushal, S, Cideciyan, AV, Schwartz, SB, Wang, L *et al.* (2008). Treatment of leber congenital amaurosis due to RPE65 mutations by ocular subretinal injection of adeno-associated virus gene vector: short-term results of a phase I trial. *Hum Gene Ther* **19**: 979–990.
19. Campochiaro, PA, Nguyen, QD, Shah, SM, Klein, ML, Holz, E, Frank, RN *et al.* (2006). Adenoviral vector-delivered pigment epithelium-derived factor for neovascular age-related macular degeneration: results of a phase I clinical trial. *Hum Gene Ther* **17**: 167–176.
20. Lai, CM, Shen, WY, Brankov, M, Lai, YK, Barnett, NL, Lee, SY *et al.* (2005). Long-term evaluation of AAV-mediated sFlt-1 gene therapy for ocular neovascularization in mice and monkeys. *Mol Ther* **12**: 659–668.
21. MacLachlan, TK, Lukason, M, Collins, M, Munger, R, Isenberger, E, Rogers, C *et al.* (2011). Preclinical safety evaluation of AAV2-sFLT01 - a gene therapy for age-related macular degeneration. *Mol Ther* **19**: 326–334.
22. Binley, K, Widdowson, PS, Kelleher, M, de Belin, J, Loader, J, Ferrige, G *et al.* (2012). Safety and biodistribution of an equine infectious anemia virus-based gene therapy, RetinoStat<sup>®</sup>, for age-related macular degeneration. *Hum Gene Ther* **23**: 980–991.
23. ter Brake, O, 't Hooft, K, Liu, YP, Centlivre, M, von Eije, KJ and Berkhout, B (2008). Lentiviral vector design for multiple shRNA expression and durable HIV-1 inhibition. *Mol Ther* **16**: 557–564.
24. Castanotto, D, Sakurai, K, Lingeman, R, Li, H, Shively, L, Aagaard, L *et al.* (2007). Combinatorial delivery of small interfering RNAs reduces RNAi efficacy by selective incorporation into RISC. *Nucleic Acids Res* **35**: 5154–5164.
25. Grimm, D, Streetz, KL, Jopling, CL, Storm, TA, Pandey, K, Davis, CR *et al.* (2006). Fatality in mice due to oversaturation of cellular microRNA/short hairpin RNA pathways. *Nature* **441**: 537–541.
26. Martin, JN, Wolken, N, Brown, T, Dauer, WT, Ehrlich, ME and Gonzalez-Alegre, P (2011). Lethal toxicity caused by expression of shRNA in the mouse striatum: implications for therapeutic design. *Gene Ther* **18**: 666–673.
27. Maetzig, T, Galla, M, Brugman, MH, Loew, R, Baum, C and Schambach, A (2010). Mechanisms controlling titer and expression of bidirectional lentiviral and gammaretroviral vectors. *Gene Ther* **17**: 400–411.
28. Kliffen, M, Sharma, HS, Mooy, CM, Kerkvliet, S and de Jong, PT (1997). Increased expression of angiogenic growth factors in age-related maculopathy. *Br J Ophthalmol* **81**: 154–162.
29. Esumi, N, Oshima, Y, Li, Y, Campochiaro, PA and Zack, DJ (2004). Analysis of the VMD2 promoter and implication of E-box binding factors in its regulation. *J Biol Chem* **279**: 19064–19073.
30. Kachi, S, Binley, K, Yokoi, K, Umeda, N, Akiyama, H, Muramatsu, D *et al.* (2009). Equine infectious anemia viral vector-mediated codelivery of endostatin and angiostatin driven by retinal pigmented epithelium-specific VMD2 promoter inhibits choroidal neovascularization. *Hum Gene Ther* **20**: 31–39.
31. Cai, Y, Bak, RO, Krogh, LB, Staunstrup, NH, Moldt, B, Corydon, TJ *et al.* (2014). DNA transposition by protein transduction of the piggyBac transposase from lentiviral Gag precursors. *Nucleic Acids Res* **42**: e28.
32. Aparicio, S, Sawant, S, Lara, N, Barnstable, CJ and Tombran-Tink, J (2005). Expression of angiogenesis factors in human umbilical vein endothelial cells and their regulation by PEDF. *Biochem Biophys Res Commun* **326**: 387–394.
33. Kitamura, T, Asai, N, Enomoto, A, Maeda, K, Kato, T, Ishida, M *et al.* (2008). Regulation of VEGF-mediated angiogenesis by the Akt/PKB substrate Girdin. *Nat Cell Biol* **10**: 329–337.
34. Hassel, D, Cheng, P, White, MP, Ivey, KN, Kroll, J, Augustin, HG *et al.* (2012). MicroRNA-10 regulates the angiogenic behavior of zebrafish and human endothelial cells by promoting vascular endothelial growth factor signaling. *Circ Res* **111**: 1421–1433.
35. Bai, YJ, Huang, LZ, Xu, XL, Du, W, Zhou, AY, Yu, WZ *et al.* (2012). Polyethylene glycol-modified pigment epithelial-derived factor: new prospects for treatment of retinal neovascularization. *J Pharmacol Exp Ther* **342**: 131–139.
36. Okamoto, S, Amaishi, Y, Goto, Y, Ikeda, H, Fujiwara, H, Kuzushima, K *et al.* (2012). A Promising Vector for TCR Gene Therapy: Differential Effect of siRNA, 2A Peptide, and Disulfide Bond on the Introduced TCR Expression. *Mol Ther Nucleic Acids* **1**: e63.
37. Yáñez-Muñoz, RJ, Balaggan, KS, MacNeil, A, Howe, SJ, Schmidt, M, Smith, AJ *et al.* (2006). Effective gene therapy with nonintegrating lentiviral vectors. *Nat Med* **12**: 348–353.
38. Jakobsen, M, Stenderup, K, Rosada, C, Moldt, B, Kamp, S, Dam, TN *et al.* (2009). Amelioration of psoriasis by anti-TNF-alpha RNAi in the xenograft transplantation model. *Mol Ther* **17**: 1743–1753.
39. Corydon, TJ, Bross, P, Holst, HU, Neve, S, Kristiansen, K, Gregersen, N *et al.* (1998). A human homologue of Escherichia coli ClpP caseinolytic protease: recombinant expression, intracellular processing and subcellular localization. *Biochem J* **331** (Pt 1): 309–316.
40. Corydon, TJ, Hansen, J, Bross, P and Jensen, TG (2005). Down-regulation of Hsp60 expression by RNAi impairs folding of medium-chain acyl-CoA dehydrogenase wild-type and disease-associated proteins. *Mol Genet Metab* **85**: 260–270.



This work is licensed under a Creative Commons Attribution-NonCommercial-NoDerivs 3.0 Unported License. The images or other third party material in this article are included in the article's Creative Commons license, unless indicated otherwise in the credit line; if the material is not included under the Creative Commons license, users will need to obtain permission from the license holder to reproduce the material. To view a copy of this license, visit <http://creativecommons.org/licenses/by-nc-nd/3.0/>